Breast Ultrasound Computer-Aided Diagnosis Using BI-RADS Features[1]

Wei-Chih Shen, MS, Ruey-Feng Chang, PhD, Woo Kyung Moon, MD, Yi-Hong Chou, MD, Chiun-Sheng Huang, MD

Rationale and Objectives. Based on the definitions in mass category of Breast Imaging Reporting and Data System developed by American College of Radiology, eight computerized features including shape, orientation, margin, lesion boundary, echo pattern, and posterior acoustic feature classes are proposed.

Materials and Methods. Our experimental database consists of 265 pathology-proven cases including 180 benign and 85 malignant masses. The capacity of each proposed feature in differentiating malignant from benign masses was validated by Student's *t* test and the correlation between each proposed feature and the pathological result was evaluated by point biserial coefficient. Binary logistic regression model was used to relate all proposed features and pathological result as a computer-aided diagnosis (CAD) system. The diagnostic value of each proposed feature in the CAD system was further evaluated by the feature selection methods. Additionally, the likelihood of malignancy for each individual feature was also estimated by binary logistic regression.

Results. On each proposed feature, the malignant cases were significantly different from the benign ones. The correlation between the angular characteristic and pathological result was indicated as very high. Three substantial correlations appear in features irregular shape, undulation characteristic, and degree of abrupt interface, but the relationship for orientation feature is low. For the constructed CAD system, the performance indices accuracy, sensitivity, specificity, PPV, and NPV were 91.70% (243 of 265), 90.59% (77 of 85), 92.22% (166 of 180), 84.62% (77 of 91), and 95.40% (166 of 174), respectively, and the area index in the ROC analysis was 0.97. Compared with the significant contribution of angular characteristic, the diagnostic values of posterior acoustic feature and orientation feature were relatively low for the CAD system. When three or more angular characteristics are discovered or the degree of abrupt interface is lower than 18, the likelihood of malignancy could be predicted as greater than 40%.

Conclusion. The computerized BI-RADS sonographic features conform to the sign of malignancy in the clinical experience and efficiently help the CAD system to diagnose the mass.

Key Words. Breast cancer; BI-RADS; ultrasound; computer-aided diagnosis (CAD) system; binary logistic regression model.

Acad Radiol 2007; 14:928–939

[1] From the Department of Computer Science and Information Engineering, National Chung Cheng University, Chiayi, Taiwan 621, R.O.C. (W.-C.S., R.-F.C.); Department of Computer Science and Information Engineering, Graduate Institute of Biomedical Electronics and Bioinformatics, National Taiwan University, Taipei, Taiwan 10617, R.O.C. (R.-F.C.); Department of Radiology and Clinical Research Institute, Seoul National University Hospital, Seoul, Korea (W.K.M.); Department of Radiology, Taipei Veterans General Hospital, National Yang Ming University School of Medicine, Taipei, Taiwan (Y.-H.C.); and Department of Surgery, National Taiwan University Hospital and College of Medicine, National Taiwan University, Taipei, Taiwan (C.-S.H.). Received February 17, 2007; accepted April 21, 2007. **Address correspondence to** R.-F.C.: e-mail: rfchang@csie.ntu.edu.tw

doi:10.1016/j.acra.2007.04.016

Breast cancer is ranked as the second leading cause for cancer death in women after lung cancer by American Cancer Society (1). The most useful way to reduce cancer deaths is early detection and treatment (2,3). The introduction of mammography into medical usage helps physicians capture the visualized information in patients' anatomy. Recently, ultrasound becomes an important alternative equipment for mammography in the evaluation of breast cancer because of its characteristics, including being noninvasive, more efficient, relatively inexpensive, real-time, and convenient (4,5). Today, the developments of imaging techniques refine the quality of pictures and can greatly improve diagnostic accuracy for early detecting breast lesions so as to reduce the number of unnecessary biopsies (6).

In the clinical diagnosis, feature detection plays a fundamental role in describing mass characteristics and could greatly affect the diagnostic result. Stavros et al. (7) proposed several sonographic characteristics to describe a mass, such as ellipsoid shape, number of lobulations, ratio of wide to anteroposterior dimension, and posterior shadowing. With the rapid development of computer applications, most imaging tools rely on a computer-aided diagnosis (CAD) system to efficiently process the digitized data. Furthermore, a powerful function in differentiating malignant from benign lesions was developed and embedded into CAD system to assist the doctors in many researches (8–29). Recently, Medipattern (Toronto, Canada) has also developed the first medical imaging software application, B-CAD, for analysis of the breast ultrasound images. In order to describe a mass in the computer system, the sonographic features are quantified into computerized sonographic features. For describing the formation of a mass, shape and margin characteristic classes could be adopted. The mass shape could be described by the moments and Fourier descriptors (8) or several factors such as roundness, aspect-ratio, convexity, and solidity (9). Madabhushi et al. (10) and Kim et al. (11) evaluated the shape irregularity by the direction of gradient magnitude and the derivative of curvature on each pixel of mass boundary, respectively. Joo et al. (12) counted the spiculate characteristic of margin class by applying the Fourier transform on the polar coordinates constructed by the boundary pixels and the center of mass. Chen et al. (13) counted the number of substantial protuberances and depressions on the margin by the convex hull. In addition to describing the mass formation, Drukker et al. (14) detected the potential lesions based on expected mass shape and margin characteristics. Except for the formation of a mass, the correlation or dissimilarity between pixels of selected ROI or a mass are also useful to describe the mass characteristics. Texture analysis is a useful method to describe such features within selected ROI or a mass (15–19). Kim et al. (20) described acoustic differences within a mass by the distribution of gray scales. Furthermore, they evaluated the degree of definition of boundary by the gradient magnitudes. For estimating the clearness degree of mass boundary, Sehgal et al. (21) partitioned the lesion boundary into N sectors and then comparing the difference significance between the inside and the outside of each sector. Horsch et al. (22) partitioned the area behind a mass into three areas and the differences between these areas are used to measure the posterior acoustic feature.

The Breast Imaging Reporting and Data System (BI-RADS) developed by the American College of Radiology standardizes the descriptions and the assessment of clinical findings (23). In the mass category, the dominant sonographic characteristics of a mass are grouped into shape, orientation, margin, lesion boundary, echo pattern, and posterior acoustic feature classes. For each feature classes, some descriptive terms are defined to help the radiologists for grading the clinical findings. Costantini et al. (24) evaluated the reliability between the radiologists' grading and the pathological result. In their results, the typical signs of malignancy were irregular shape, antiparallel orientation, noncircumscribed margin, echogenic halo, and decreased sound transmission. The grades of BI-RADS sonographic characteristics associated with patient's medical history, Baker et al. (25), or associated with patient age, Lo et al. (26), could be used to construct a CAD system by artificial neural network. Further, the reliability between the predicted results of CAD system and the clinical decision to perform biopsy of five radiologists were discussed by Baker et al. (27). In these results, the CAD system using the evaluations of BI-RADS sonographic characteristics efficiently improves interpretation of abnormalities for radiologists. Besides, Markey et al. (28) showed that calcification affects the diagnostic performance of CAD system diagnosed by the evaluations of BI-RADS sonographic characteristics. Therefore, mass and calcification should be considered separately when the CAD system is applied. The advantage for the CAD system using the evaluations of BI-RADS sonographic characteristics is that the CAD system could be applied on the different ultrasound systems (29).

The purpose of this study was to quantify all feature classes defined in the mass category of BI-RADS into

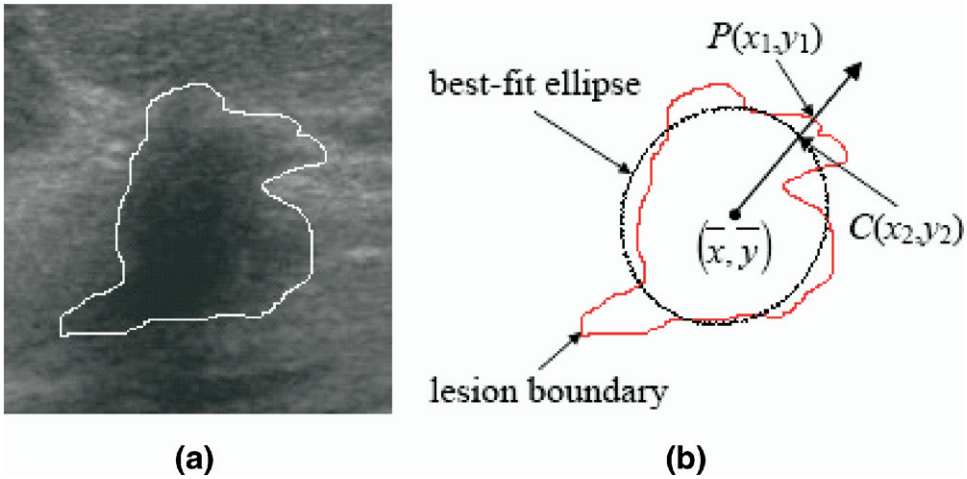

Figure 1. The descriptive terms for mass shape include oval, round, and irregular in BI-RADS. (**a**) A malignant mass. (**b**) The irregular degree of mass shape is estimated by the dissimilarity between lesion boundary and corresponding best-fit ellipse in computerized BI-RADS features.

eight computerized features. The pathological result was regarded as a gold standard in capability evaluations and diagnostic performance measurements related to the proposed computerized BI-RADS features. The objectives of our study was to develop comprehensive features as the radiologists' grading. That is, the behaviors of the proposed features were expected to conform to the typical sign of malignancy in clinical experiences. A CAD system would be constructed by a binary logistic regression model (30). The diagnostic value of each computerized BI-RADS feature was further evaluated by the feature selection methods during the constructing process of CAD system. Additionally, two critical thresholds would be defined to detect high likelihood of malignancy for an immediate warning signal to radiologists.

MATERIALS AND METHODS

Data Acquisition

This study was approved by the local ethics committee, and informed consent was obtained from all included patients. Total of 265 cases were acquired by the attending radiologist using the HDI 5000 machine (Advanced Technological Laboratory, Bothell, WA) and a linear array transducer with variable frequency from 5 to 12 MHz from June to July 2004 (including 180 benign and 85 malignant breast masses). Preinterventional images were obtained in all patients. According to the definitions of assessment categories in BI-RADS, the final assessment of 265 solid breast masses on the basis of ultrasonographic findings before biopsy was category 3, probably benign lesions, for 45 masses (17%); category 4, suspicious lesions, for 180 (68%); and category 5, highly suggestive of malignancy, for 40 (15%). All the cases had been proven by pathology either with fine needle aspiration cytology or with core needle biopsy. Two radiologists with 6 and 13 years of experience, respectively, in breast imaging decided the position of lesion margin by consensus and one of radiologists drew the boundary using a paint program (Microsoft Paint, version 5.2, Microsoft Inc, Seattle, WA).

Computerized BI-RADS Features

In BI-RADS, the descriptive terms for describing the dominant sonographic characteristics of a mass are standardized and grouped into six classes: shape, orientation, margin, lesion boundary, echo pattern, and posterior acoustic feature. Eight computerized BI-RADS features are proposed to quantify these sonographic characteristics as follows.

Shape Class

The best-fit ellipse (31) could be used to roughly describe the mass shape as shown in Figure 1 and regarded as baseline for measuring the degree of irregular shape. For any pixel $P(x_1, y_1)$ on the lesion boundary, a crossing pixel $C(x_2, y_2)$ on the best-fit ellipse is found by a ray that starts at the center of best-fit ellipse. The dissimilarity between $P(x_1, y_2)$ and $C(x_2, y_2)$ is then evaluated by their distance

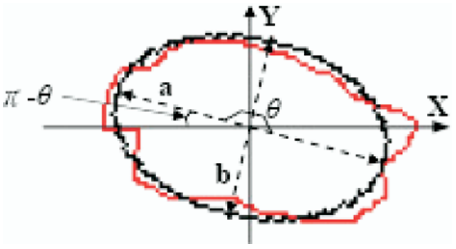

Figure 2. The descriptive terms for mass orientation include parallel and not parallel in BI-RADS. The orientation of mass could be measured by the angle of major axis of best-fit ellipse in computerized BI-RADS features.

$$D(P) = \sqrt{(x_1 - x_2)^2 + (y_1 - y_2)^2}. \quad (1)$$

Finally, the shape feature S_V is estimated by the dissimilarity between mass shape and best-fit ellipse as

$$S_V = \frac{\sum_{P \in LB} D(P)}{LB_N} \quad (2)$$

where P is any pixel on the lesion boundary and LB_N denotes the number of pixels on the lesion boundary.

Orientation Class

The orientation of a mass could also be measured by the angle of major axis of above best-fit ellipse as shown in Figure 2. For measuring the parallel degree, the range of mass orientation should be defined between 0 and $\frac{\pi}{2}$. However, the acquired angle of major axis of best-fit ellipse θ does not always conform to this property as shown in Figure 2. Therefore, the orientation feature O_E is defined by adjusting the acquired θ into the range 0 and $\frac{\pi}{2}$ as

$$O_E = \begin{cases} \theta & if \ 0 \le \theta \le \frac{\pi}{2} \\ \pi - \theta & if \ \frac{\pi}{2} < \theta \le \pi \\ \theta - \pi & if \ \pi < \theta \le \frac{3\pi}{2} \\ 2\pi - \theta & if \ \frac{3\pi}{2} < \theta \le 2\pi \end{cases}. \quad (3)$$

Margin Class

The distance map (31) could be used to capture the undulation and the angular characteristics of mass margin. For any pixel $P(x, y)$ in the ROI, its eight neighbors are defined as

$$N_8(P) = \{(x-1, y-1), (x, y-1), (x+1, y-1), (x-1, y), (x+1, y), (x-1, y+1), (x, y+1), (x+1, y+1)\} \quad (4)$$

The distance from P to the lesion boundary is recursively defined as

$$Distance(P) = Min\{Distance(N_8(P))\} + 1 \quad (5)$$

where $Min\{Distance(N_8(P))\}$ denotes the minimum of known distance in P's eight neighbors. The distance for all boundary pixels are set to 0 as initial condition. An example for illustrating distance map is shown in Figure 3b and 3c. Then, a maximum inscribed circle inside the mass is found to extract the margin features from the distance map. By the maximum inscribed circle, some lobulate areas are clearly partitioned from the mass as shown in Figure 3d. However, only the significant lobulate areas should be counted. Therefore, if the maximum distance within lobulate area is less than four, such area is regarded as slighter undulation and should be ignored. Then, the number of significant lobulate areas is defined as the undulation characteristics M_U of margin class. Furthermore, the local maxima on the distance map could be used to detect the angular characteristics as shown in Figure 3e. In order to count the number of angular characteristics M_A, the local maxima in each lobulate area are grouped by their Euclidean coordinates as shown in Figure 3f. In the grouping algorithm, the Euclidean distances from a new discovered local maximum to the center of each formed grouped local maxima are calculated. If the shortest distance is larger than a predefined threshold, the new discovered local maximum is regarded as a new grouped local maximum. Whereas, the new discovered local maximum is appended to the grouped local maxima which with the shortest distance and then the center of the modified grouped local maxima is recalculated. By experimentation, the predefined threshold is set to 10 in this study. In the grouping algorithm, those local maxima within the maximum inscribed circle would be ignored. For example, the local maxima located in the upper of

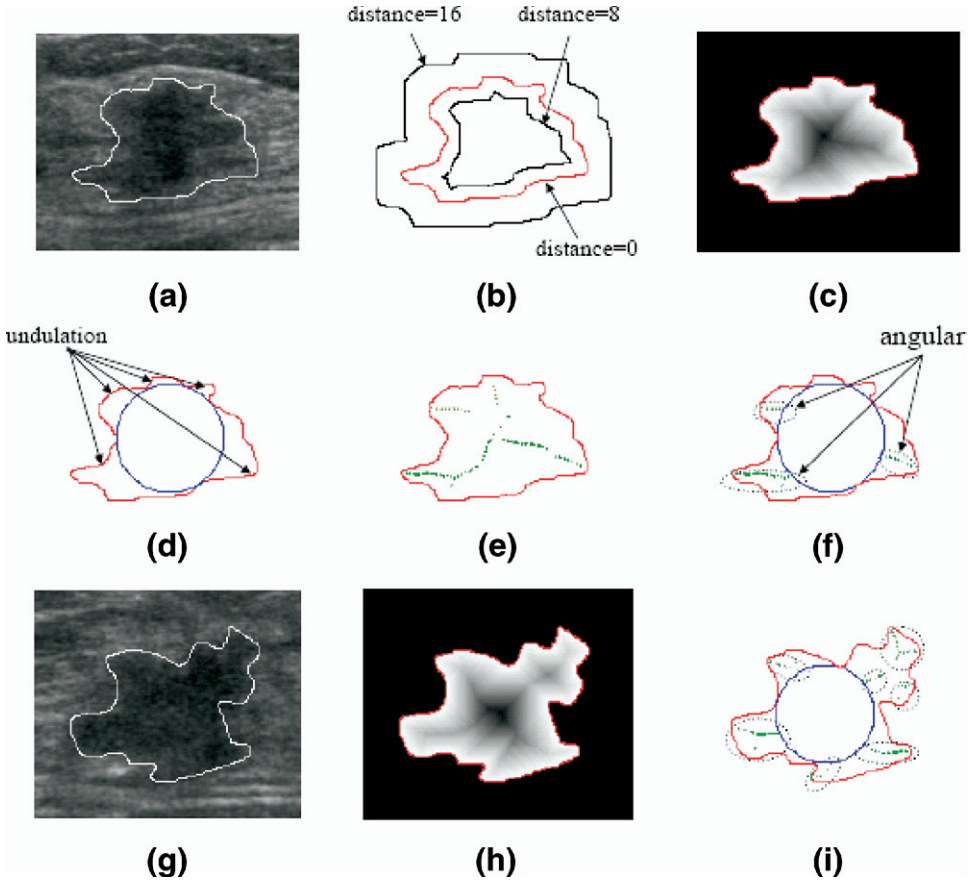

Figure 3. The descriptive terms for not circumscribed mass margin include indistinct, angular, microlobulated, and spiculated in BI-RADS. The selected ROI is transformed into the distance map for capturing the undulation and the angular characteristics of margin class in computerized BI-RADS features. (**a**) A malignant lesion. (**b**) The distance map of (**a**). (**c**) The distance map of mass is represented by the gray scales. The black color denotes the farthest distance to the lesion boundary. (**d**) Five undulation characteristics are explored. (**e**) The local maxima could be used to detect the angular characteristics. (**f**) Three angular characteristics are explored. (**g**) A malignant lesion. (**h**) The distance map of (**g**). (**i**) Seven angular characteristics are explored.

mass were ignored as shown in Figure 3e. Compared with the feature M_U, the feature M_A especially detects the angular characteristics on the margin as shown in Figure 3i.

Lesion Boundary Class

For estimating the degree of abrupt interface across the lesion boundary, the distance map could be used to partition part of the surrounding tissue and the outer mass, which are both adjacent to the lesion boundary as shown in Figure 4. In the figure, part of surrounding tissue and the outer mass consist of the pixels, each of which the distance is less than 11, respectively. The average gray intensities of these two areas with width k are respectively defined as

$$avg_{Tissue} = \frac{\sum_{distance(P)=1}^{k} I(P)}{N_{Tissue}} \quad \text{and} \quad avg_{Mass} = \frac{\sum_{distance(P)=1}^{k} I(P)}{N_{Mass}} \tag{6}$$

where $I(P)$ is the gray intensity of pixel P, N_{Tissue} denotes the number of pixels in the partitioned part of surrounding tissue, and N_{Mass} represents the number of pixels in the outer mass. Then, the lesion boundary feature LB_D for evaluating the degree of abrupt interface is defined as

$$LB_D = avg_{Tissue} - avg_{Mass}. \tag{7}$$

By experimentation, the width k is set to 3 in this study.

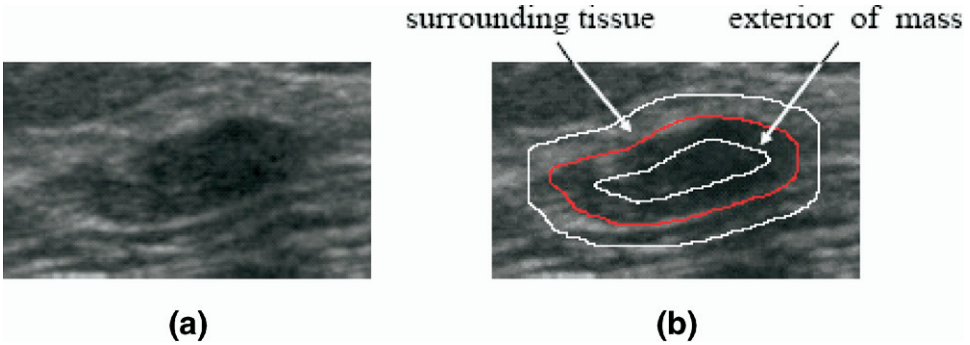

Figure 4. The descriptive terms for the lesion boundary of a mass include abrupt interface and echogenic halo in BI-RADS. The degree of abrupt interface across the lesion boundary is estimated by the color difference between the surrounding tissue and the outside of the mass in computerized BI-RADS features.

Echo Pattern Class

The average gray intensity and the variation of mass are used to represent the echo pattern features, respectively. The average gray intensity EP_I is defined as

$$EP_I = \frac{\sum_{P \in Mass} I(P)}{N_{Mass}} \tag{8}$$

where $I(P)$ is the gray intensity of mass pixel P and N_{Mass} denotes the number of mass pixels.

The variation on pixel P could be estimated by the gradient magnitude. According to the definition of neighbors in Equation 4, the Sobel gradients (31) on x-direction and y-direction of pixel $P(x, y)$ are respectively defined as

$$\begin{aligned} G_X(P) = {} & I(x-1, y-1) + 2 * I(x-1, y) + I(x-1, y+1) \\ & - I(x+1, y-1) - 2 * I(x+1, y) - I(x+1, y+1) \end{aligned}$$

and

$$\begin{aligned} G_Y(P) = {} & I(x-1, y-1) + 2 * I(x, y-1) \\ & + I(x+1, y-1) - I(x-1, y+1) \\ & - 2 * I(x, y+1) - I(x+1, y+1). \end{aligned} \tag{9}$$

Then, the gradient magnitude on P is defined as

$$G(P) = \sqrt{G_X(P)^2 + G_Y(P)^2} \tag{10}$$

Finally, the internal echo pattern feature EP_{AG} could be estimated by the average variation as

$$EP_{AG} = \frac{\sum_{P \in Mass} G(P)}{N_{Mass}}. \tag{11}$$

Posterior Acoustic Feature Class

For measuring the posterior acoustic feature, a posterior area is defined behind the mass as shown in Figure 5. The width of the posterior area is defined by two-thirds of the mass width. At both sides of posterior area, a gap which has one-sixth of the mass width is preserved for avoiding the edge shadowing. The height of posterior area is equal to the mass height but does not exceed 100 pixels. The average gray intensity of the posterior area is defined as

$$avg_{PA} = \frac{\sum_{P \in PA} I(P)}{N_{PA}} \tag{12}$$

where $I(P)$ is the gray intensity of pixel P in the posterior area and N_{PA} denotes the number of pixels in the posterior area. Then, the posterior acoustic feature PS_D is defined as

$$PS_D = avg_{PA} - EP_I \tag{13}$$

where EP_I is defined in Equation 8.

Experimental Method and Performance Evaluation

Each computerized BI-RADS feature will be evaluated by two different methods. At first, the capability

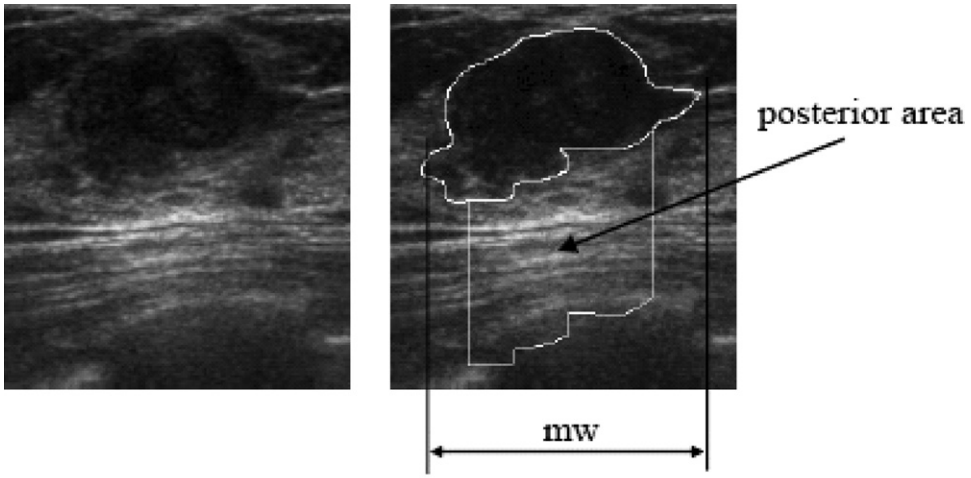

Figure 5. The descriptive terms for the posterior acoustic feature of a mass include no posterior acoustic features, enhancement, shadowing, and combined pattern in BI-RADS. (**a**) A malignant mass. (**b**) The definition of the posterior area. The difference between the average gray intensity of a mass and that of defined posterior area is calculated to measure the posterior acoustic feature in the computerized BI-RADS features.

in differentiating benign from malignant lesions will be evaluated by Student's t test. Furthermore, the relationship between pathological result and each computerized BI-RADS feature is estimated by point biserial correlation coefficient symbolized as r_{pb} (32). In the interpretation of the resulting coefficient, r_{pb} can range from 0 to 1 if two scales are related positively and from 0 to -1 if two scales are related negatively. Further, the absolute value of r_{pb} could reflect the strength of correlation. The magnitude value between 0.01 and 0.09 was considered as negligible; 0.10–0.29, low; 0.30–0.49, moderate; 0.50–0.69, substantial; 0.70–0.99, very high; 1.0, perfect (32).

The k-fold cross-validation method (33) is used to verify the performance of CAD system. In this study, $k = 10$, the adopted cases were randomly partitioned into 10 sets according to the pathological result. The numbers of benign and malignant cases in each set is similar. Each set is regarded as the test set one time and diagnosed by the CAD system constructed by the remaining nine sets. Finally, the diagnostic results in the 10 test sets were merged. When the pathological result is regarded as gold standard, the diagnostic performance could be evaluated by five performance indices including accuracy, sensitivity, specificity, positive predictive value (PPV), and negative predictive value (NPV) and defined as:

$$\begin{aligned}
&\text{Accuracy} = (\text{TP} + \text{TN})/(\text{TP} + \text{TN} + \text{FP} + \text{FN}),\\
&\text{Sensitivity} = \text{TP}/(\text{TP} + \text{TN}),\\
&\text{Specificity} = \text{TN}/(\text{TN} + \text{FP}),\\
&\text{PPV} = \text{TP}/(\text{TP} + \text{FP}), \text{and}\\
&\text{NPV} = \text{TN}/(\text{TN} + \text{FN}).
\end{aligned} \tag{14}$$

where TP is the number of positives correctly classified as positive, TN is the number of negatives correctly classified as negative, FP is the number of negatives falsely classified as positive, and FN is the number of positives falsely classified as negative. Moreover, the ROC analysis is also used to evaluate the diagnostic performance. The ROCKIT software (C. Metz, University of Chicago, Chicago, IL) is used in the ROC analysis.

The feature selection method could be also used to observe the diagnostic value of each computerized BI-RADS feature in the CAD system. Two major feature selection methods, forward entered and backward removed (30), will be adopted in the paper. In the forward entered method, the feature with the most contribution for predicting the likelihood of malignancy is considered for inclusion prior to construct a new CAD system at each step. In the backward removed method, all features are involved to construct a CAD system at beginning, and then going back and deleting the feature that does not contribute significantly at each step. At each step, the

Table 1
Mean Values and Standard Deviations (SDs) for the Benign and Malignant Groups

Class	Feature	Mean ± SD		*P* value	r_{pb}
		Benign	Malignant		
Shape	S_V	16.75 ± 19.19	126.78 ± 130.49	<.001	0.56
Orientation	O_E	11.93 ± 13.33	15.93 ± 17.75	<.05	0.12
Margin	M_U	2.16 ± 0.87	3.52 ± 1.17	<.001	0.56
	M_A	1.61 ± 1.01	4.56 ± 2.09	<.001	0.70
Lesion boundary	LB_D	27.29 ± 10.45	13.18 ± 7.93	<.001	−0.57
Echo pattern	EP_I	49.69 ± 13.82	39.09 ± 14.12	<.001	−0.35
	EP_{AG}	48.30 ± 10.86	37.32 ± 8.59	<.001	−0.46
Posterior shadowing	PS_D	42.02 ± 19.82	26.23 ± 27.12	<.001	−0.32

The significance for differentiating the benign from malignant group is verified by the Student's *t* test. The strength of relationship between the pathological result and each proposed BI-RADS feature is evaluated by the point-biserial correlation coefficient r_{pb}.

strength of relationship between the pathological result and the constructed CAD system could be estimated by R^2 statistic (30). The resulting R^2 value ranges from 0 to 1, and a larger value denotes a stronger correlation. Moreover, during the feature selection, the improvement of constructed CAD system compared with that in the previous step could be estimated by χ^2 statistic (30). The resulting χ^2 value represents the benefit for selecting or removing such feature.

In order to provide an immediate warning to radiologists, even without a full CAD system, the diagnostic function is specifically constructed for each individual computerized BI-RADS feature and the corresponding likelihood of malignancy on the different feature evaluation is calculated. According to the specific likelihood, a critical threshold could be defined. When the feature evaluation conflicts the critical threshold, the radiologists should be reminded with high possibility of malignance immediately.

RESULTS

Data Analysis of Computerized BI-RADS Features

The mean value and the standard deviation of each computerized BI-RADS feature on the benign and malignant groups were listed in Table 1. According to the Student's *t* test, the benign group was statistically different from the malignant group on each computerized BI-RADS feature because all *P* values are less than .001 or .05. Four correlations between the features S_V, O_E, M_U, and M_A and the pathological result were positive related reflected by point biserial statistic. That is, irregular shape (larger S_V), not parallel orientation (larger O_E), more undulation characteristics (larger M_U), and more angular characteristics (larger M_A) all indicate a higher likelihood of malignancy. The signs of the point biserial statistic results in the remaining features were negative. That is, abrupt interface of lesion boundary (larger LB_D), brighter lesion (larger EP_I), complex internal echo pattern (larger EP_{AG}), and enhancement of posterior area (larger PS_D) all indicate a lower likelihood of malignancy. Additionally, the strength of correlation could be measured by the absolute value of the coefficient. The correlation between the angular characteristic of margin class and the pathological result was indicated as very high ($r_{pb} = 0.70$). Three substantial correlations appeared in features S_V, M_U, and LB_D, but the relationship for orientation feature O_E was indicated as low.

Computer-Aided Diagnosis Using All Computerized BI-RADS Features

At first, the performance of CAD system using all proposed features will be evaluated. The distributions of the likelihoods of malignancy in the diagnosis result could be observed by a histogram as shown in Figure 6. The histogram bin width was set to 0.05, and the numbers of benign and malignant cases were calculated. Clearly, most of malignant cases were predicted with a higher likelihood of malignancy and most of benign cases were predicted with a lower likelihood of malignancy. Further, the ROC analysis was applied on the final result and the area index (Az) is 0.97 as shown in Figure 7.

According to the result of ROC analysis, the threshold for deciding whether a lesion is benign or malignant was defined to 0.4. The diagnostic result and performance

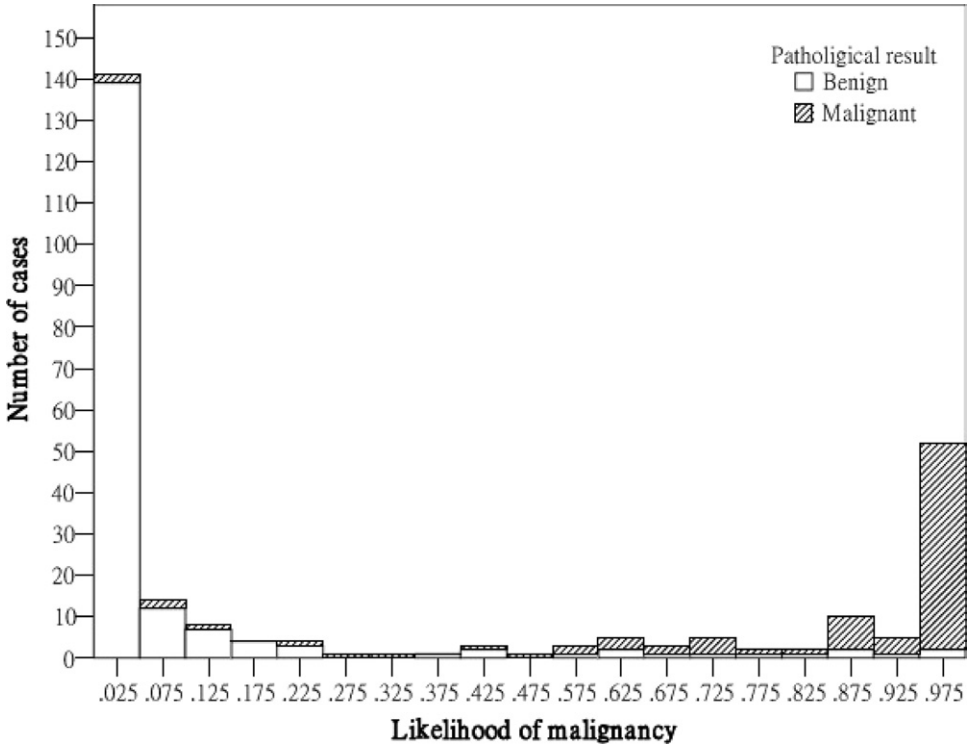

Figure 6. The histograms for showing the frequency of predicted likelihood of malignancies on benign and malignant groups.

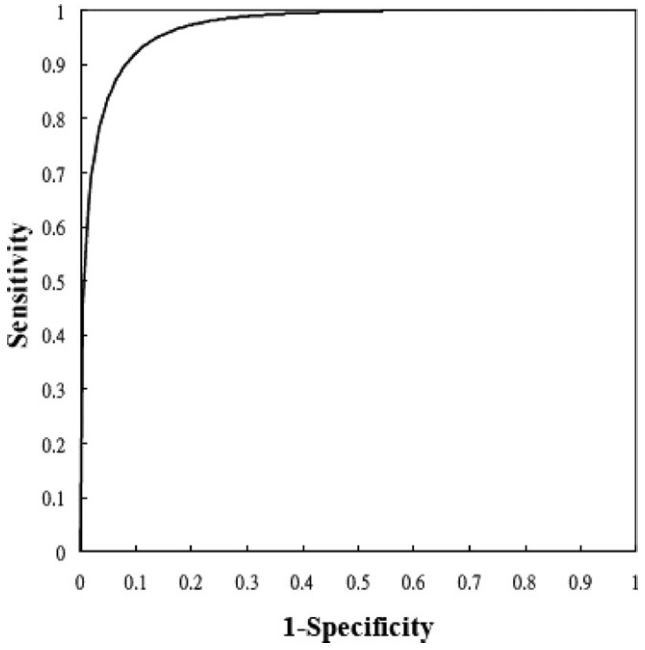

Figure 7. The ROC curves for CAD systems using all computerized BI-RADS features and the area index (Az) is 0.97.

Table 2
The Diagnostic Result of the CAD System

	CAD system		
Pathology	Benign	Malignant	Total
Benign	TN 166	FP 14	180
Malignant	FN 8	TP 77	85
Total	174	91	265

were listed in Tables 2 and 3, respectively. The performance indices accuracy, sensitivity, specificity, PPV, and NPV were 91.70% (243 of 265), 90.59% (77 of 85), 92.22% (166 of 180), 84.62% (77 of 91), 95.40% (166 of 174), respectively.

DISCUSSION

Diagnostic Value of Each Computerized BI-RADS Feature in the CAD System

The entering and removing order in the feature selection methods could be used to observe the diagnostic value of each computerized BI-RADS feature as listed in

Table 3
The Diagnostic Performance of the CAD System

Performance indices	Rate
Accuracy	91.70%
Sensitivity	90.59%
Specificity	92.22%
PPV	84.62%
NPV	95.40%

Table 4. In the forward entered method, the angular characteristic M_A of margin class was entered at the first step. When features were stepwise entered, the capability of constructed CAD system was obviously improved until step 5. However, the improvement began to slow down from steps 5 to 8. In the backward removed method, all features were used to construct a CAD system at beginning. From steps 2 to 4, the damage to the CAD system was slight even though three features are removed. The capability of constructed CAD system began to decrease at step 5, and the angular characteristic M_A of margin class was removed at the last step. According to these results, the angular characteristic M_A of margin class was the most significant feature for the CAD system because it is always entered at the beginning and removed at the last step. Besides, the contributions of orientation characteristic O_E and posterior shadowing characteristic PS_D for CAD system were relatively negligible in all computerized BI-RADS features. Besides, the entering and removing order positively related to the strength of correlation of the point biserial results in Table 1. The feature with larger correlation strength was generally entered at earlier and removed at later.

Critical Thresholds on Angular and Degree of Abrupt Interface Characteristics

Because angular characteristic M_A and degree of abrupt interface characteristic LB_D are the most significant features proved in the above experiments, two critical thresholds would be defined. From the diagnostic function for angular characteristic M_A as shown in Figure 8a, the slope of function was steep when three or four angular characteristics are discovered. The critical threshold could be defined to three because the likelihood of malignancy is greater than 40%. If a mass with three or more angular characteristics is predicted as malignant, the diagnostic performance indices accuracy, sensitivity, specificity, PPV, and NPV were 86.42% (229 of 265), 87.06% (74 of 85), 86.11% (155 of 180), 74.75% (74 of 99), and 93.37% (155 of 166), respectively.

In the diagnostic function of the degree of abrupt interface LB_D as shown in Figure 8b, as the increasing of sharp degree, the likelihood of malignancy was progressively decreased. When the feature value LB_D is equal to or larger than 18, the likelihood of malignancy is smaller than 40%. The critical threshold for LB_D was therefore set to 18. If a mass is predicted as malignant if its evaluation of feature LB_D is smaller than 18, the diagnostic performance indices accuracy, sensitivity, specificity, PPV, and NPV were 79.62% (211 of 265), 72.94% (62 of 85), 82.78% (149 of 180), 66.67% (62 of 93), and 86.63% (149 of 172), respectively.

Although all performance indices for the predicted function using feature M_A or using feature LB_D were lower than that using all computerized BI-RADS features, the likelihood of malignancy for each individual proposed BI-RADS feature could be observed. When the evaluation of an individual feature is greater than a predefined threshold, an immediate warning could be provided to radiologists even with a full CAD system.

CONCLUSION AND FUTURE WORKS

The BI-RADS sonographic characteristics including shape, orientation, margin, lesion boundary, echo pattern, and posterior acoustic feature classes are quantified into eight computerized features in this study. These computerized BI-RADS features are significant in differentiating malignant from benign masses and highly correlate to the pathological result. For the constructed CAD system, the angular characteristic in margin class is the most significant feature. However, the diagnostic value of posterior acoustic feature and orientation feature are relatively lower. Except for the CAD system using all proposed computerized BI-RADS features, warning signal could be defined by an individual feature to the radiologists. When three or more angular characteristics are discovered or the degree of abrupt interface is lower than 18, the likelihood of malignancy could be predicted greater than 40%.

In the future, threes subjects would be performed. First, the reliability of mass sonographic characteristics between the grades of radiologists and the evaluations of computerized BI-RADS features would be discussed. Further, the differences of diagnostic performances between the CAD system using the grades of radiologists and that using the computerized BI-RADS features would be com-

Table 4
The Diagnostic Value of Each Proposed Feature in the Diagnosis Function is Verified by the Feature Selection Methods

	Forward selected			Backward removed		
Step	Feature	R^2	χ^2	Feature	R^2	χ^2
1	M_A	0.657	167.980	All	0.851	248.588
2	LB_D	0.731	27.870	O_E	0.851	−0.008
3	EP_I	0.779	19.675	PS_D	0.850	−0.533
4	M_U	0.805	11.474	EP_I	0.847	−1.747
5	S_V	0.845	18.709	M_U	0.830	−7.870
6	EP_{AG}	0.850	2.339	S_V	0.784	−20.641
7	PS_D	0.851	0.533	EP_{AG}	0.731	−21.939
8	O_E	0.851	0.008	LB_D	0.657	−27.870
9				M_A		−167.980

When the feature is selected or removed at each step, the R^2 value indicates ability of CAD system for predicting the pathological result and the improvement compared to the previous step is evaluated by the χ^2.

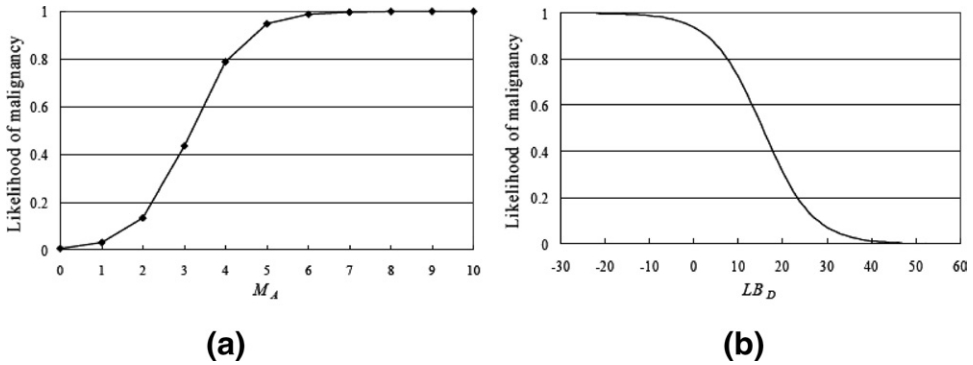

Figure 8. The diagram for evaluating the likelihood of malignancy. (**a**) The angular characteristic. (**b**) The degree of abrupt interface.

pared. Second, an automatic mass segmentation method will be introduced into our CAD system. The correlation between two evaluations for applying the computerized BI-RADS features on the automatic segmented result and on the manually decided mass would be evaluated. When the automatic segmented result is close to the manually decided mass, their correlation should be reflected as highly positive related. Third, radiologists classify the clinical finding into BI-RADS assessment category according to the estimating likelihood of malignancy in the clinical diagnosis. A computer aided classification system would be developed for automatically classifying the lesions in to BI-RADS assessment category using the proposed computerized BI-RADS features.

REFERENCES

1. Jemal A, Siegel R, Ward E, et al. Cancer statistics, 2006. CA Cancer J Clin 2006; 56:106–130.
2. American Cancer Society. Cancer Facts and Figures 2006. American Cancer Society, Atlanta, GA 2006.
3. American Cancer Society. Cancer Prevention & Early Detection Facts & Figures 2006. American Cancer Society, Atlanta, GA 2006.
4. Baker JA, Soo MS. Breast US: Assessment of technical quality and image interpretation. Radiology 2002; 223:229–238.
5. Rizzatto GJ. Towards a more sophisticated use of breast ultrasound. Eur Radiol 2001; 11:2425–2435.
6. Williams JC. US of solid breast nodules. Radiology 1996; 198:585.
7. Stavros At, Thickman D, Rapp CL, et al. Solid breast nodules: Use of sonography to distinguish between benign and malignant lesions. Radiology 1995; 196:123–134.
8. Liang S, Rangayyan RM, Desautels JEL. Application of shape analysis to mammographic calcifications. IEEE Trans Med Imaging 1994; 13: 263–274.
9. Chang RF, Wu WJ, Moon WK, et al. Automatic ultrasound segmentation and morphology based diagnosis of solid breast tumors. Breast Cancer Res Treat 2005; 89:179–185.
10. Madabhushi A, Metaxas DN. Combining low-, high-level and empirical domain knowledge for automated segmentation of ultrasonic breast lesions. IEEE Trans Med Imaging 2003; 22:155–169.
11. Kim KG, Cho SW, Min SJ, et al. Computerized scheme for assessing ultrasonographic features of breast masses. Acad Radiol 2005; 12: 58–66.
12. Joo S, Yang YS, Moon WK, et al. Computer-aided diagnosis of solid breast nodules: Use of an artificial neural network based on

multiple sonographic features. IEEE Trans Med Imaging 2004; 23:1292–1300.
13. Chen CM, Chou YH, Han KC, et al. Breast lesions on sonograms: Computer-aided diagnosis with nearly setting-independent features and artificial neural networks. Radiology 2003; 226:504–514.
14. Drukker K, Giger ML, Vyborny CJ, et al. Computerized detection and classification of cancer on breast ultrasound. Acad Radiol 2004; 11: 526–535.
15. Chang RF, Wu WJ, Moon WK, et al. Support vector machines for diagnosis of breast tumors on US images. Acad Radiol 2003; 10: 189–197.
16. Chen DR, Chang RF, Huang YL. Computer-aided diagnosis applied to US of solid breast nodules by using neural networks. Radiology 1999; 213:407–412.
17. Chang RF, Wu WJ, Moon WK, et al. Improvement in breast tumor discrimination by support vector machines and speckle-emphasis texture analysis. Ultrasound Med Biol 2003; 29:679–686.
18. Chen DR, Chang RF, Huang YL, et al. Texture analysis of breast tumors on sonograms. Semin Ultrasound CT MR 2000; 21:308–316.
19. Bader W, Bohmer S, van LP, et al. Does texture analysis improve breast ultrasound precision? Ultrasound Obstet Gynecol 2000; 15:311–316.
20. Kim KG, Kim JH, Min BG. Classification of malignant and benign tumors using boundary characteristics in breast ultrasonograms. J Digit Imaging 2002; 15(suppl 1):224–227.
21. Sehgal CM, Cary TW, Kangas SA, Weinstein SP, Schultz SM, Arger PH, Conant EF. Computer-based margin analysis of breast sonography for differentiating malignant and benign masses. J Ultrasound Med 2004; 23(9):1201–1209.
22. Horsch K, Giger ML, Venta LA, Vyborny CJ. Computerized diagnosis of breast lesions on ultrasound. Med Phys 2002; 29(2): 157–164.
23. American College of Radiology. Breast Imaging Reporting and Data System, 4th ed. American College of Radiology, 2003.
24. Costantini M, Belli P, Lombardi R, et al. Characterization of solid breast masses: Use of the sonographic breast imaging reporting and data system lexicon. J Ultrasound Med 2006; 25(5):649–659.
25. Baker JA, Kornguth PJ, Lo JY, Williford ME, Floyd CE Jr. Breast cancer: prediction with artificial neural network based on BI-RADS standardized lexicon. Radiology 1995; 196:817–822.
26. Lo JY, Baker JA, Kornguth PJ, Iglehart JD, Floyd CE Jr. Predicting breast cancer invasion with artificial neural networks on the basis of mammographic features. Radiology 1997; 203:159–163.
27. Baker JA, Kornguth PJ, Lo JY, Floyd CE Jr. Artificial neural network: improving the quality of breast biopsy recommendations. Radiology 1996; 198:131–135.
28. Markey MK, Lo JY, Floyd CE Jr. Differences between computer-aided diagnosis of breast masses and that of calcifications. Radiology 2002; 223:489–493.
29. Bilska-Wolak AO, Floyd CE Jr, Lo JY, Baker JA. Computer aid for decision to biopsy breast masses on mammography: Validation on new cases. Acad Radiol 2005; 12:671–680.
30. Hosmer DW, Lemeshow S. Applied Logistic Regression, 2nd ed. New York: Wiley, 2000.
31. Jain AK. Fundamentals of Digital Image Processing. Englewood Cliffs, NJ: Prentice-Hall, 1989.
32. Davis JA. Elementary survey analysis. Englewood Cliffs, NJ: Prentice-Hall, 1971.
33. Stone M. Cross-validatory choice and assessment of statistical predictors. J R Stat Soc B 1974; 36:111–147.